

Supplementary Materials: *In-situ* synchrotron X-ray thermodiffraction of boranes

Pascal G. Yot, Philippe Miele and Umit B. Demirci

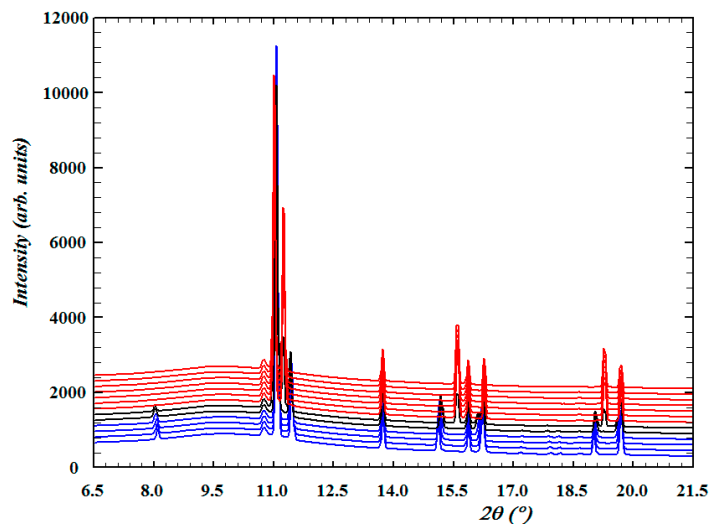


Figure S1. Waterfall plots of a fragment of the diffraction patterns of AB collected upon heating showing the phase transition. The patterns in blue, black and red correspond to low-temperature AB (orthorhombic, s.g. $Pnm21$), a mixture of low-temperature and high-temperature AB, and high-temperature AB (tetragonal, s.g. $I4mm$), respectively.

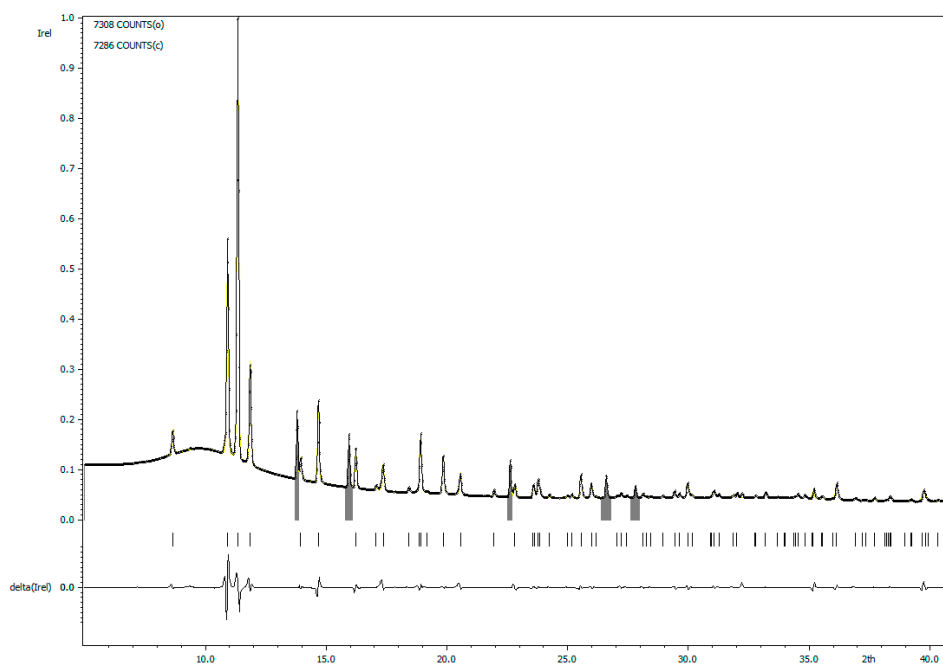


Figure S2. Structure-independent refinement of the unit cell of the diffraction pattern obtained for AB (orthorhombic, s.g. $Pnm21$) at 81 K (GoF = 32.42, R_p = 1.81, wR_p = 3.35).

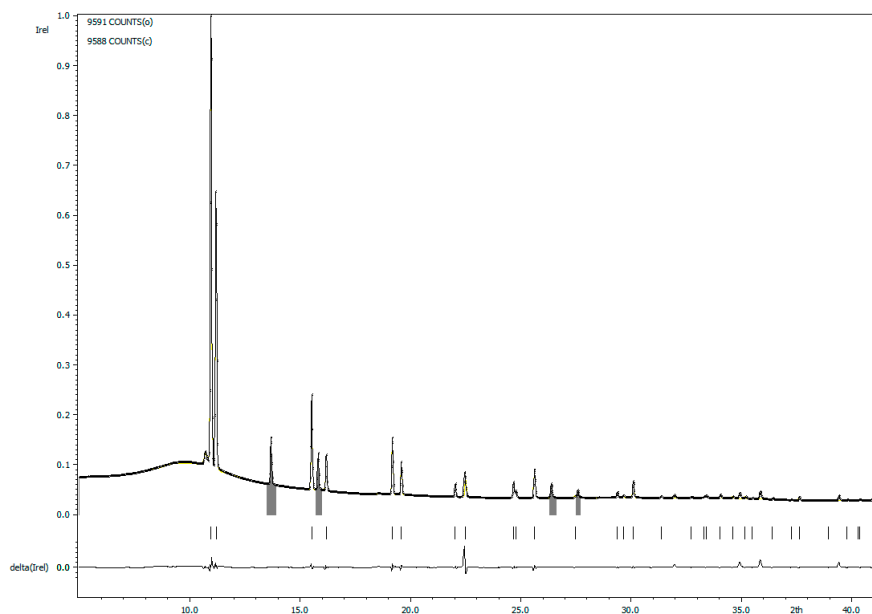


Figure S3. Structure-independent refinement of the unit cell of the diffraction pattern obtained for AB (tetragonal, s.g. $I4mm$) at 295 K (GoF = 49.24, Rp = 1.53, wRp = 5.11).

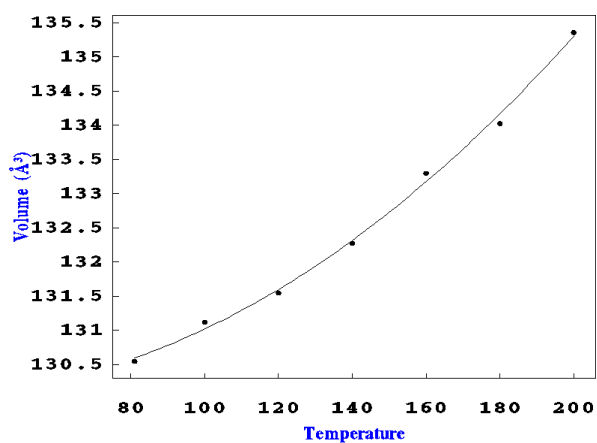


Figure S4. Evolution of the unit cell volume for the low-temperature phase of AB (orthorhombic, s.g. $Pmm21$) as a function of the temperature.

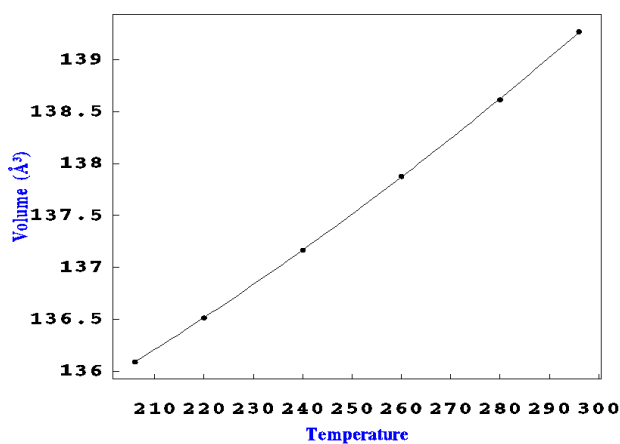


Figure S5. Evolution of the unit cell volume for the high-temperature phase of AB (tetragonal, s.g. $I4mm$) as a function of the temperature.

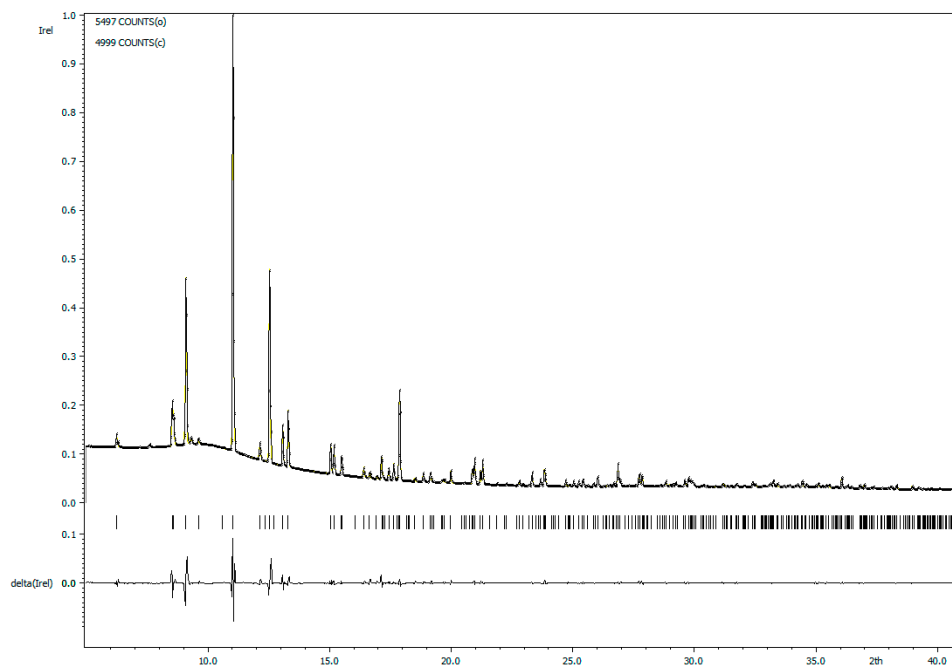


Figure S6. Structure-independent refinement of the unit cell of the diffraction pattern obtained for HB (orthorhombic, s.g. *Pbcn*) at 101 K (GoF = 20.05, Rp = 1.84, wRp = 2.69).

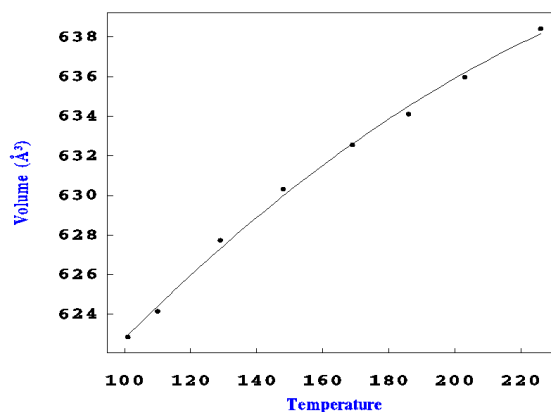


Figure S7. Evolution of the unit cell volume for HB (orthorhombic, s.g. *Pbcn*) as a function of the temperature, for $T < 240$ K.

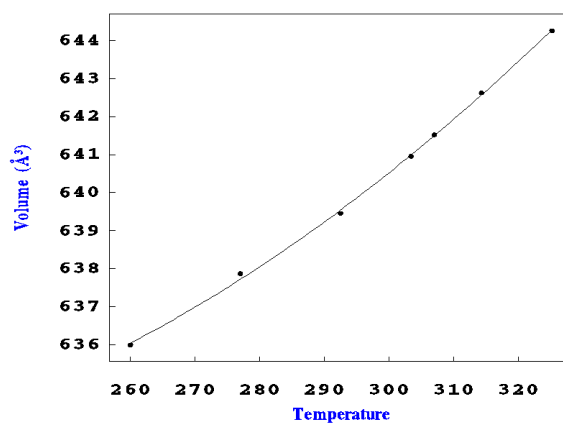


Figure S8. Evolution of the unit cell volume for HB (orthorhombic, s.g. *Pbcn*) as a function of the temperature, for $T > 240$ K.

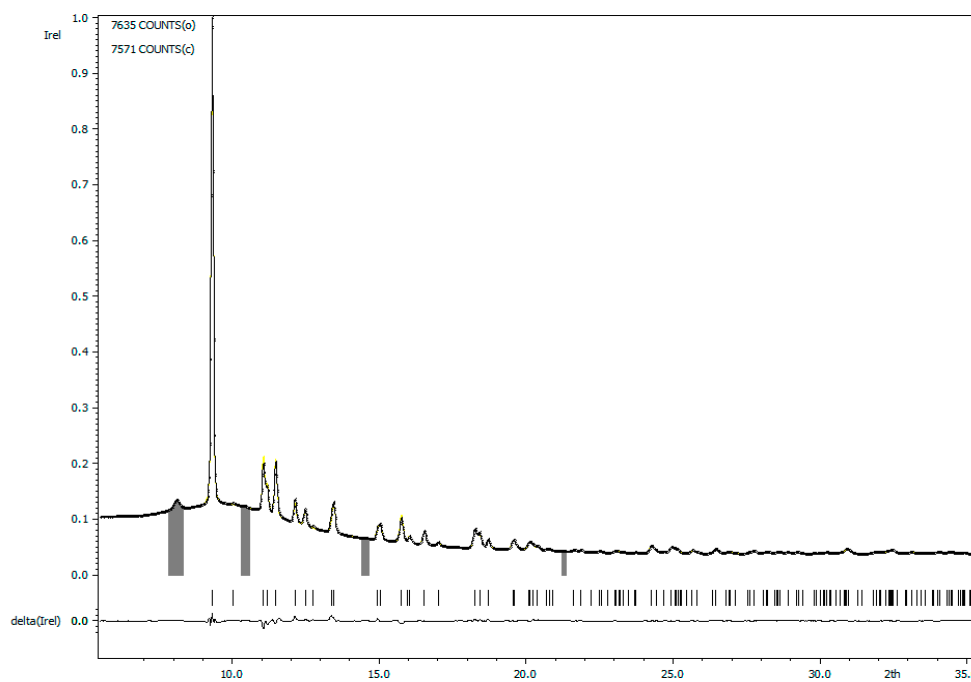


Figure S9. Structure-independent refinement of the unit cell of the diffraction pattern obtained for HBB (orthorhombic, s.g. *Pbca*) at 81 K (GoF = 10.64, Rp = 0.94, wRp = 1.20).

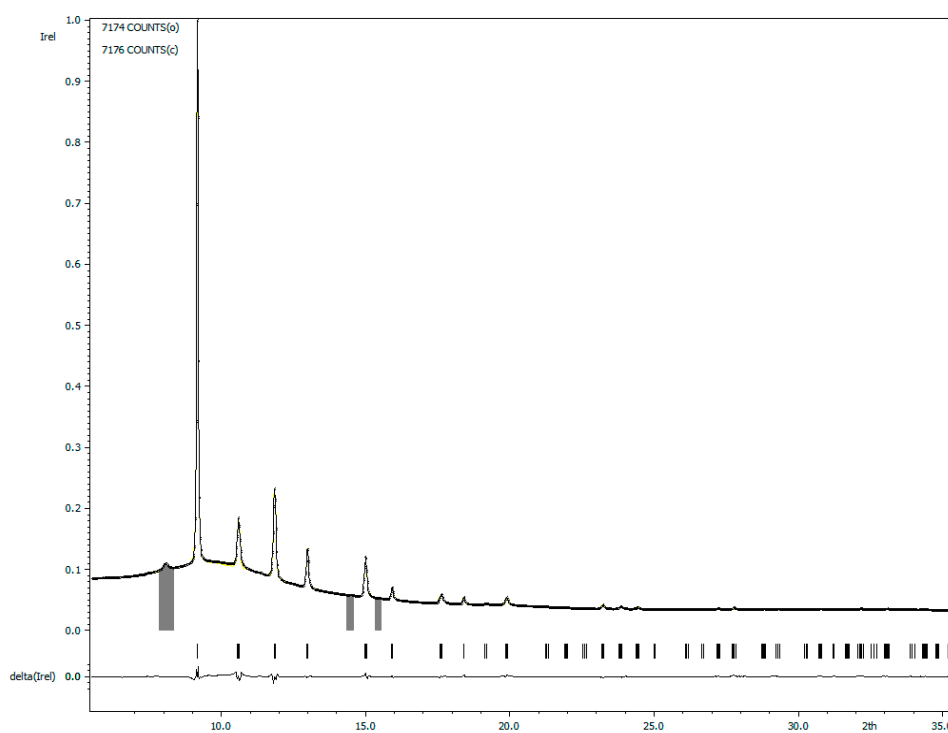


Figure S10. Structure-independent refinement of the unit cell of the diffraction pattern obtained for HBB (orthorhombic, s.g. *Pbca*) at 311 K (GoF = 9.06, Rp = 0.97, wRp = 1.14).

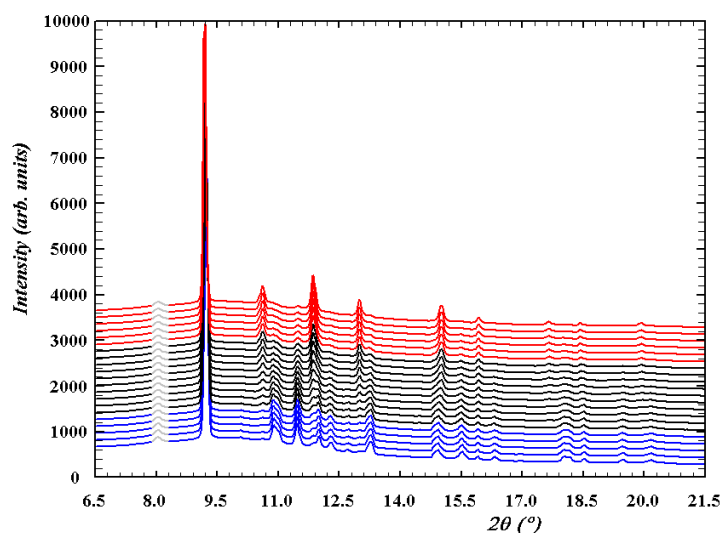


Figure S11. Waterfall plots of a fragment of the diffraction patterns of HBB (orthorhombic, s.g. *Pbca*) collected upon heating. The patterns in red, black, and blue correspond respectively to high-temperature HBB, a mixture, and low-temperature HBB.

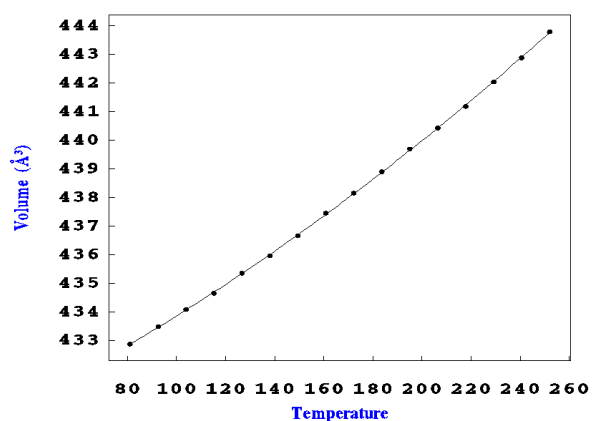


Figure S12. Evolution of the unit cell volume for the low-temperature phase of HBB (orthorhombic, s.g. *Pbca*) as a function of the temperature.

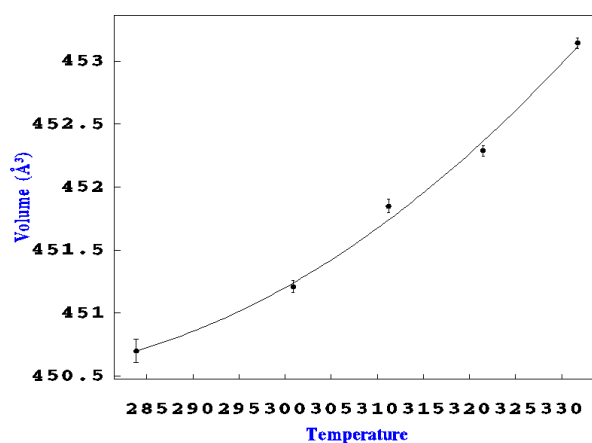


Figure S13. Evolution of the unit cell volume for the high-temperature phase of HBB (orthorhombic, s.g. *Pbca*) as a function of the temperature.

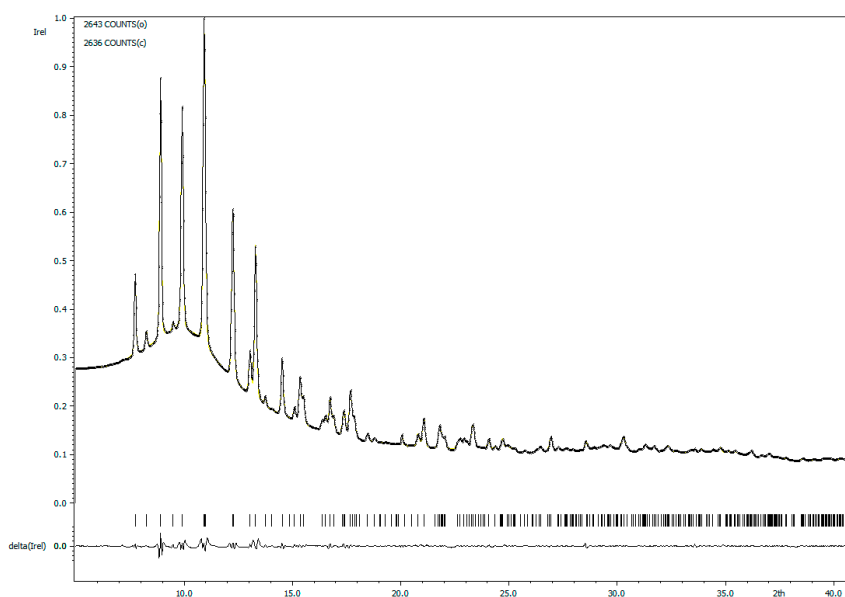


Figure S14. Structure-independent refinement of the unit cell of the diffraction pattern obtained for LiHB (monoclinic, s.g. $P21/c$) at 81 K (GoF = 7.32, Rp = 0.65, wRp = 0.81).

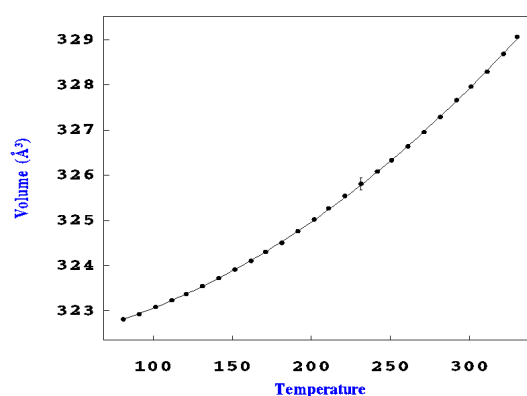


Figure S15. Evolution of the unit cell volume for LiHB (monoclinic, s.g. $P21/c$) as a function of the temperature.

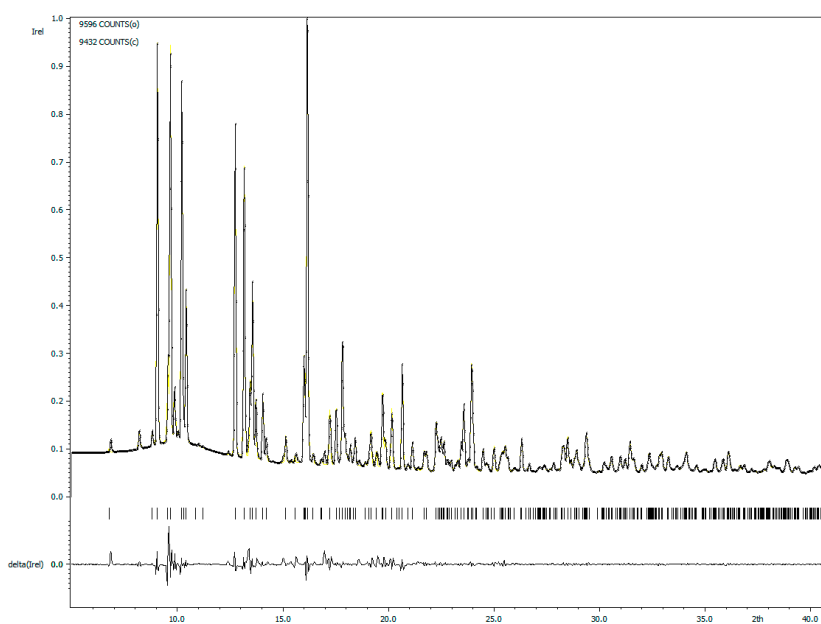


Figure S16. Structure-independent refinement of the unit cell of the diffraction pattern obtained for NaHB (monoclinic, s.g. $P21/n$) at 81 K (GoF = 40.52, Rp = 2.19, wRp = 3.00).

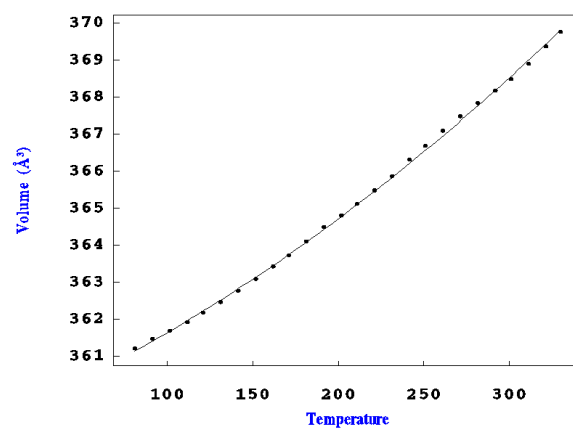


Figure S17. Evolution of the unit cell volume for NaHB (monoclinic, s.g. P21/n) as a function of the temperature.

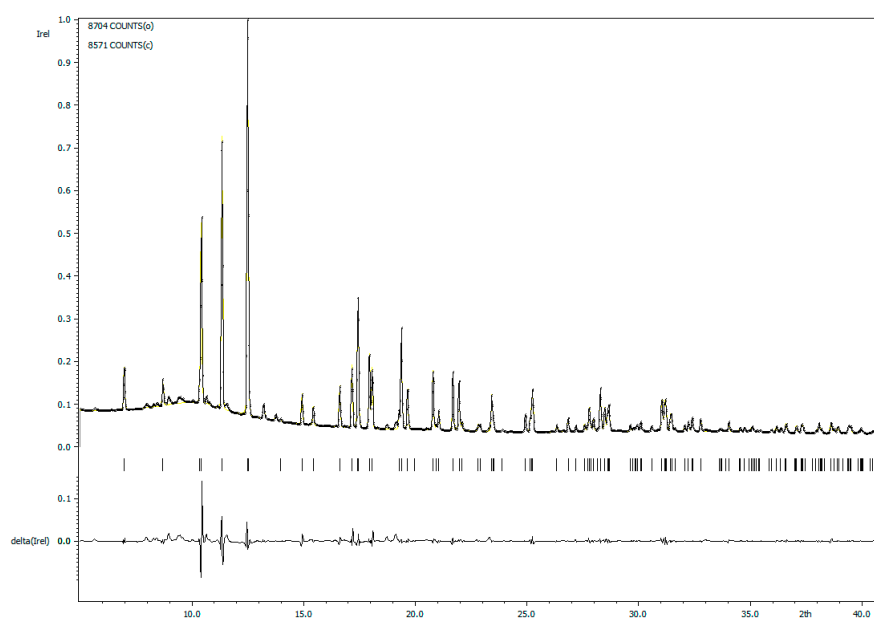


Figure S18. Structure-independent refinement of the unit cell of the diffraction pattern obtained for STB (orthorhombic, s.g. *Pmm21*) at 81 K (GoF=42.05, Rp=3.25, wRp=4.09).

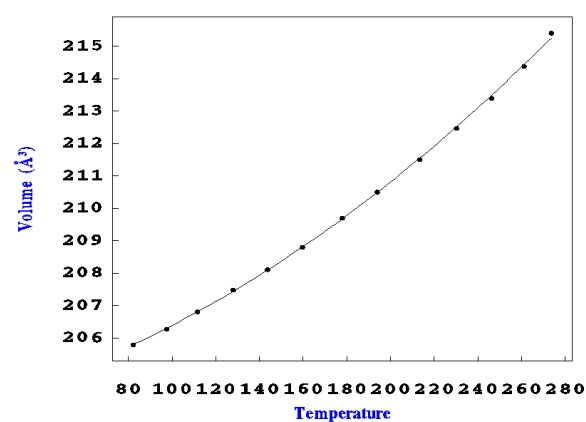


Figure S19. Evolution of the unit cell volume for NaHB ((orthorhombic, s.g. *Pmm21*) as a function of the temperature.